A SIMPIFIED PREDICTION METHOD FOR SEISMIC RESPONSES OF BUILDING FRAME STRUCTURES ALLOWED TO UPLIFT

Tatsuya Azuhata[1] and Tadashi Ishihara[2]

[1] International Institute of Seismology and Earthquake Engineering, Building Research Institute
Tsukuba, 305-0802, Ibaraki
e-mail: azuhata@kenken.go.jp

[2] Department of Production Engineering, Building Research Institute
Tsukuba, 305-0802, Ibaraki
e-mail: tishihar@kenken.go.jp

Keywords: Uplift, Rocking, Earthquake Response Reduction, Higher Modes, Response Spectrum.

Abstract. *Previous studies cleared that rocking behaviors can reduce seismic damages of some buildings. Based on this knowledge, some rocking structural systems which are allowed to uplift during earthquakes intentionally have been proposed as one of seismic energy dissipation systems. In this study, we propose a simplified prediction method for earthquake responses of such rocking structural systems.*

To predict earthquake responses of the rocking systems, we need to evaluate effects of higher modes. We consider there are two sources to generate higher modes in the rocking systems. When a building starts uplift, higher modes simultaneously occur due to vertical inertial effects in the superstructure. Therefore, a dynamic overturning moment of the rocking systems surpasses that estimated statically. We evaluate this effect by using solutions of a free vibration of the target structure. Initial velocity for the free vibration can be specified if a velocity response spectrum is provided and the fundamental natural period, which is elongated after uplifting is appropriately estimated. Also, higher modes occur due to high-frequency components of an input earthquake ground motion. If the high-frequency components of the input motion are relatively large, performance for earthquake response reduction of the rocking structural system may deteriorate. These higher modes excited by the high-frequency components can be evaluated by using the response spectrum, too. We predict maximum earthquake responses of the rocking structural systems by combining the solution of free vibrations and higher mode responses of the corresponding fixed base model.

1 INTRODUCTION

Previous studies cleared that rocking behaviors can reduce seismic damages of some buildings [For examples, 1-4]. Based on this knowledge, some rocking structural systems which are allowed to uplift during earthquakes intentionally have been proposed as one of seismic energy dissipation systems [For examples, 5-13]. In this study, we propose a simplified prediction method for earthquake responses of such rocking structural systems.

To predict earthquake responses of the rocking systems, we need to evaluate effects of higher modes. We consider there are two sources to generate higher modes in the rocking systems. When a building starts uplift, higher modes simultaneously occur according to vertical dynamic motion in the superstructure [1, 14, 15]. Therefore, a dynamic overturning moment of the rocking systems surpasses that estimated statically as shown in Fig.1.

$$Q_{up} = 0.5MgB / H$$
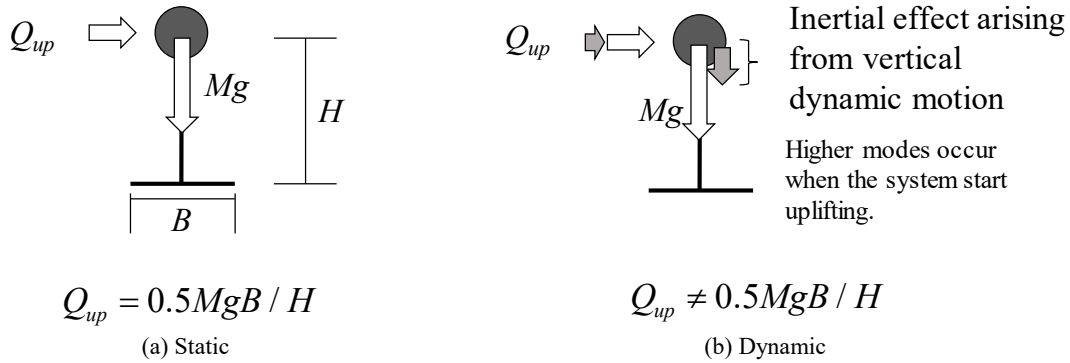
$$Q_{up} \neq 0.5MgB / H$$

(a) Static (b) Dynamic

Figure 1: Inertial effect arising from vertical dynamic motion in rocking system

Also, higher modes occur due to high-frequency components of an input earthquake ground motion. If the high-frequency components of the input motion are relatively large, performance for earthquake response reduction of the rocking structural system may deteriorate [3].

We investigate such two effects of higher modes to seismic responses of rocking structural systems by free vibration analyses in chapter 3 and discuss a simplified method to predict seismic responses of them in chapter 4.

2 ANALYSIS MODEL AND TIME HISTORY RESPONSE ANALYSIS

2.1 System considered

In this study, we simulate earthquake responses of a frame allowed to uplift using a lumped mass system shown in Fig. 2. The height of superstructure is 30m and the width is footing beam is 7.5m. This system has two vertical springs under the footing beam. These springs can sustain only a compressive force. Initially, deformations of these springs are negative due to an effect of the self-wait of the system. When the deformation of either spring becomes zero under seismic loading, the system starts uplifting. The sway displacement is constrained. And we do not consider yielding of the super structure in this study. Mass of all mass points is equal. The story stiffness increases linearly from top to base. The ratio of stiffness of the top story to that of the base story is 0.5. These mass and stiffness of the superstructure are set so that the natural first period of it is equal to 1.0s.

The equations of motion of the system in horizontal, rotational and vertical directions are shown as the following Eq. (1) - (3), respectively.
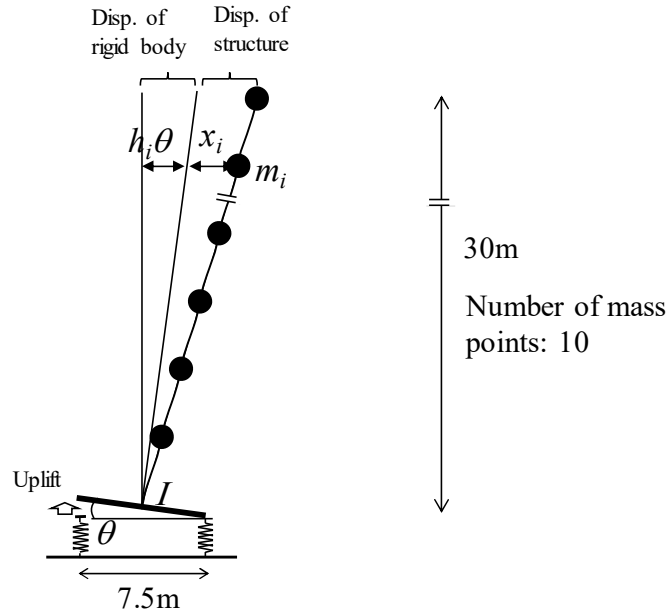
Figure 2: Lamped mass system for analyses

$$[M]\{\ddot{x}\}+[M]\{h_i\}\ddot{\theta}+[C]\{\dot{x}\}+[K]\{x\}=-[M]\{1\}\ddot{x}_g \qquad (1)$$

$$\{h_i\}^T[M]\{\ddot{x}\}+I\ddot{\theta}+R(t)=-\{h_i\}^T[M]\{1\}\ddot{x}_g \qquad (2)$$

$$\sum m\ddot{z}+V(t)=-\sum mg \qquad (3)$$

where, $[M]$, $[C]$ and $[K]$: mass, damping and stiffness matrices of the super structure respectively, $\{h_i\}$: column vector consisting of height of each mass point, I: inertial moment of the footing beam, which is neglected in this study, Σm: Total mass of the system, $R(t)$ and $V(t)$: rotational and vertical restoring forces by vertical springs under the footing beam.

We compose the $[C]$ matrix setting damping factors, h_i, for all natural modes of the super structure to 2%.

The stiffness of soil springs varies according to the contact condition, that is whether the system is uplifting or not. Thus, $R(t)$ and $V(t)$ in Eq. (2) and (3) are affected by this condition. To make responses with impact stable, we include slight damping forces, which is probably negligible to comprehensive response characteristics, in the $R(t)$ and $V(t)$ by putting a dashpot in parallel with the spring. The dashpot is separated from the superstructure when the displacement of the vertical spring becomes zero.

T_1=1.03 sec T_2=0.36 sec T_3=0.22 sec T_4=0.16 sec $T_1=\infty$ T_2=0.37 sec T_3=0.23 sec T_4=0.21 sec

(Contact phase)   (Uplift phase)
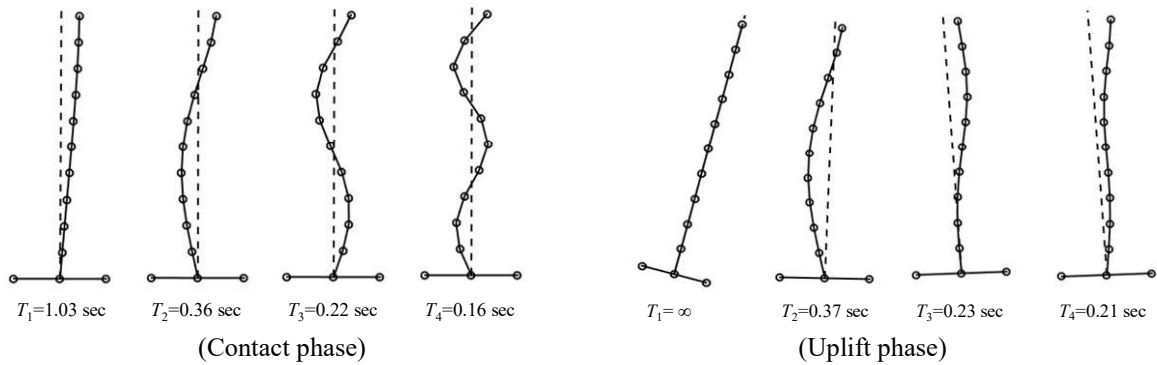
Figure 3: Natural modes and natural periods in contact and uplift phases

Figure 3 shows natural modes and natural periods of the contact and the uplift phases. The first natural period of the contact phase elongates from 1.0 s to 1.03s due to a flexibility effect of vertical springs. The first natural period of the uplift phase is infinity. The first natural mode of this phase is a rigid body mode. The second and third natural periods of the uplift phase are almost same as those of the contact phase.

2.2   Input ground motion

The input ground motion is an artificial ground motion (BCJ L2), which was proposed for structural design of high-rise buildings in Japan. The time duration is 120s and the peak ground velocity is about 0.5m/s. Velocity response spectra for two critical damping ratios, 2% and 5%, are shown in Fig.4. For free vibration analyses in chapter 3, we will use the maximum response velocity corresponding to the natural period of the contact phase estimated in this figure.
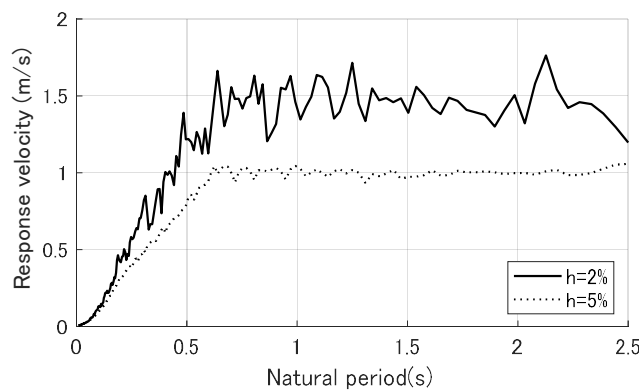

Figure 4: Velocity response spectra of input ground motion

2.3   Results of time history analysis

Figure 5 and 6 show time histories of roof displacements and uplifts on the base. The maximum roof displacement is about 70cm: the maximum uplift is about 15cm. Figure 7 shows a time history of base shear coefficient. We can see distinguished influence of higher modes to the base shear in the shape of wave. Figure 8 compares the maximum story shear coefficient of each story to that of the corresponding fixed base system. This results verify that shear forces can be reduced by allowing uplift to the structure. Figure 8 also shows the ultimate static shear forces for the rocking system by a broken line. These forces are estimated statically using seismic design lateral forces of Japanese seismic code. The dynamic results surpass the static estimation due to higher mode effects.
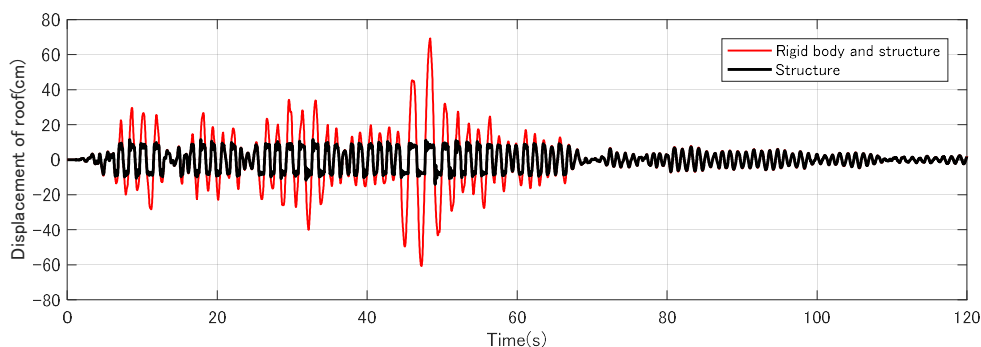

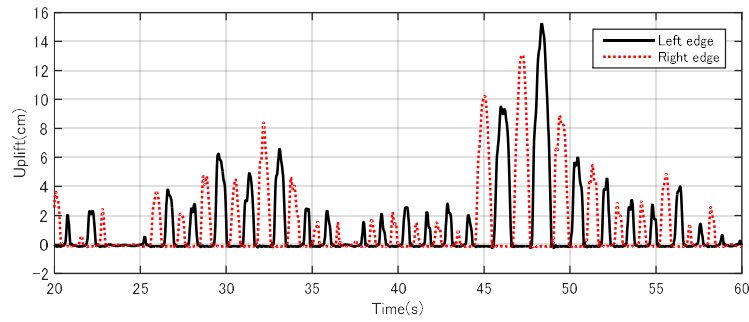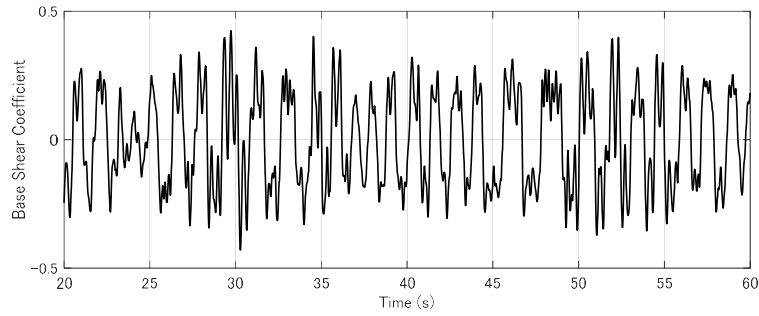Figure 5: Time history of roof displacement

Figure 6: Time history of uplift

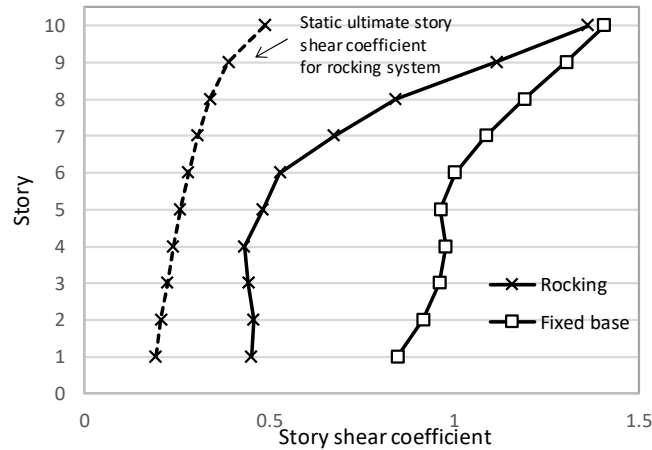Figure 7: Time history of base shear

Figure 8: Comparison of shear coefficients of rocking system with those of fixed base system

3   FREE VIBRATION ANALYSES

3.1   Analysis procedure

We conduct free vibration analyses to investigate effects of higher modes to response characteristics of the rocking system. Initial velocity $\{V_0\}$ and displacement $\{D_0\}$ of each mass point for the free vibration analysis are determined by Eq. (4) and Eq. (5) respectively.

$$\{V_0\} = \sum \beta_i \{\varphi_i\} S_{vi} \cos \theta_i \tag{4}$$

$$\{D_0\} = \sum \beta_i \{\varphi_i\} S_{vi} \sin \theta_i / \omega_{ni} \tag{5}$$

where, $\beta_i\{\varphi_i\}$: participation vector in the contact phase, S_{vi}: the maximum response velocity of the equivalent one mass system, θ_i: phase angle, ω_{ni}: natural circular frequency in the contact phase.

We use first three modes to determine initial conditions. The S_{vi} for each mode can be estimated by referring a response velocity spectra for h=2% in Fig. 2 as shown in Table 1. The first response period generally elongates when the system uplifts. However, the response velocity spectra in Fig.4 is constant in the range where natural periods are longer than 0.6s. Thus, we can neglect this elongation in this study and use the response velocity on the constant spectra as the S_{vi} of the first mode.

The phase angle of each mode is set in the two ways as shown in Table 2. From this setting, we obtain two initial conditions shown in Fig.9.

Table 1: The maximum response velocity of equivalent one-mass system for each mode

	Natural period (s)	q_{vi} (m/s)
First mode	1.03	1.50
Second mode	0.36	0.85
Third mode	0.22	0.50

Table 2: Phase angle θ_i of each mode

	First mode	Second mode	Third mode
Initial condition - 1	0	0	0
Initial condition - 2	0	$\pi/2$	$\pi/2$

Initial velocity
(a) Initial condition – 1

Initial velocity

Initial displacement
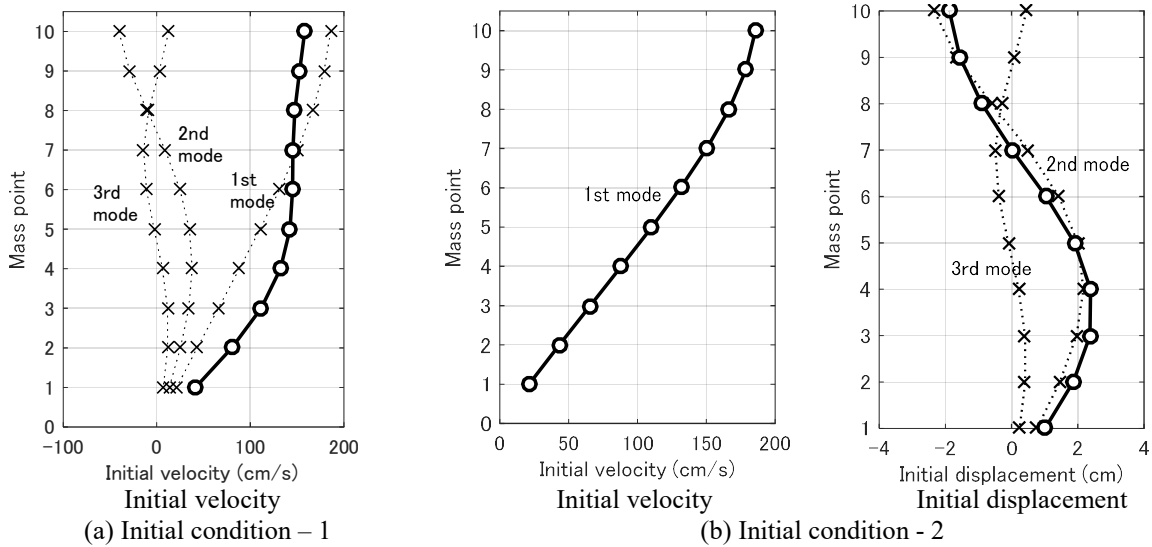(b) Initial condition - 2

Figure 9: Initial conditions for free vibration analyses

Free vibration displacement response of a linear system can be expressed by Eq. (6), (7).

$$\{D(t)\} = \sum_i \{\varphi_i\} q_{di}(t) \tag{6}$$

$$q_{di}(t) = e^{-h_i \omega_{ni} t} \left\{ q_{di}(0) \cos \omega_{di} t + \frac{q_{vi}(0) + h_i \omega_{ni} q_{di}(0)}{\omega_{di}} \sin \omega_{di} t \right\} \tag{7}$$

where,

$$\omega_{di} = \sqrt{1 - h_i^2} \, \omega_{ni} \tag{8}$$

$$q_{di}(0) = \{\varphi\}^T [M] \{D_0\} / \{\varphi\}^T [M] \{\varphi\} \tag{9}$$

$$q_{vi}(0) = \{\varphi\}^T [M] \{V_0\} / \{\varphi\}^T [M] \{\varphi\} \tag{10}$$

The uplifting system is not a linear system. However, if we divide a whole response into some piecewise linear responses in the time domain, we can apply the general solution for the free

vibration like Eq. (6) - (10) for each one [14, 15]. When the system starts uplifting from the contact phase, we need to change natural modes and frequencies to those for the uplift phase and recalculate $q_{di}(0)$ and $q_{vi}(0)$ in Eq. (6), (7). When the system lands on the ground again, we need to reconstruct Eq. (6), (7) in the same way. We apply this piecewise linear method to solve free vibration problems of the uplift system. In this study, we estimate the viscous damping factor h_i for each mode as 0.02 for all phases supposing the effect of damping forces in the $R(t)$ and $V(t)$ in Eq. (2) and (3) are negligible.

A. K. Chopra and R. K. Goel proposed the "uncoupled modal history response analysis" procedure to apply the classical modal history response analysis to non-linear systems [16]. Also, they presented the exact modal history response analysis procedure for the non-linear systems considering "the coupling of N equations in modal coordinate" [16]. We apply their concepts to free vibration analyses of the rocking system to extract effects of higher modes. The analysis procedure are as follows;

1) Separate initial conditions shown in Fig. 9 into the original three modal initial conditions which are expressed as $\beta_i\{\varphi_i\}q_{vi}\cos\theta_i$ and $\beta_i\{\varphi_i\}q_{vi}\sin\theta_i/\omega_{ni}$ in the right side of Eq. (4), (5),

2) Evaluate the separated free vibration response under each modal initial condition at the discretized analysis step,

3) Calculate summation of all separated free vibration responses to get a whole response at each step,

4) Judge whether the system starts uplifting or finishes it based on the whole response,

5) Reconstruct Eq. (6), (7) for all separated free vibration responses, if the system condition of uplifting varies,

6) Continue the analysis until response results for a sufficient time duration are obtained.

We refer to this analysis procedure as the "coupled modal free vibration analysis (CMFVA)" procedure here. Also, we refer to separated free vibration responses under the first, second and third modal initial conditions as "primary," "secondary" and "tertiary" responses respectively for convenience. These responses do not mean the pure modal responses. Especially, the primary response includes large affections by higher modes. Higher modes composing the primary response will be shown later.

3.2   Analysis results

Figures 10 to 13 compares results of the CMFVA analysis under the initial condition - 1 with those under the initial condition - 2. Figure 10 and 11 show shear coefficients of top story and base shear coefficients, respectively. In the case of the initial condition - 1, the primary, secondary and tertiary responses reach to their maximum almost simultaneously. Thus, whole responses, which are summation of all separated responses, under initial condition - 1 become larger than those under initial condition - 2.
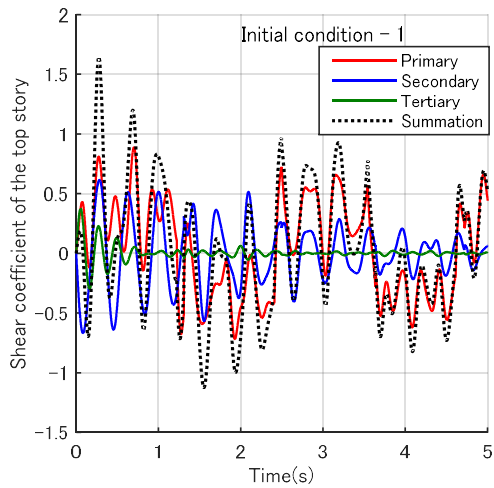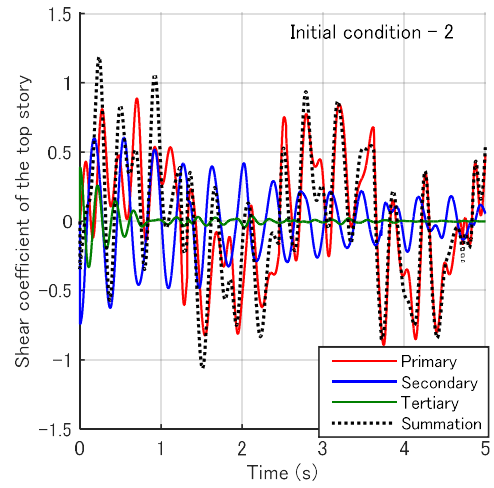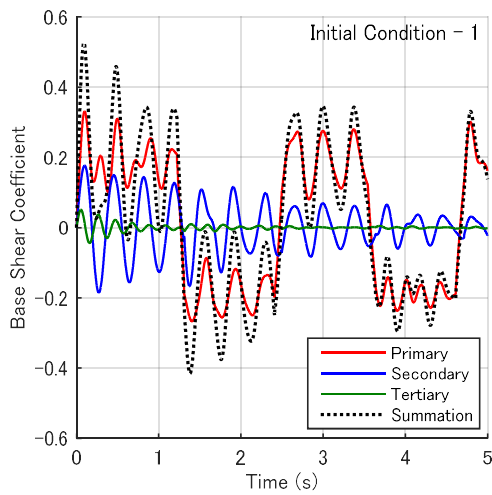
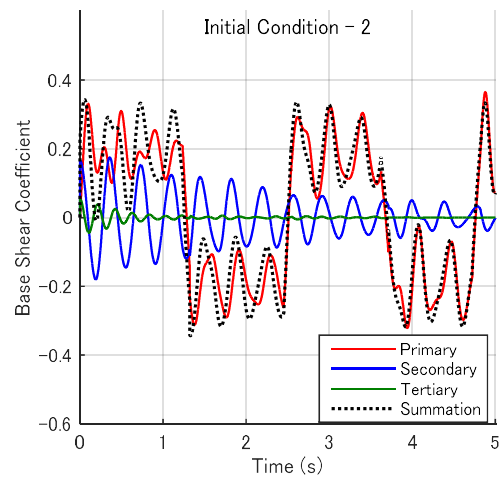(a) Initial condition - 1   (b) Initial condition - 2

Fig.10: Comparison of shear coefficients of top story under different initial conditions (CMFVA)
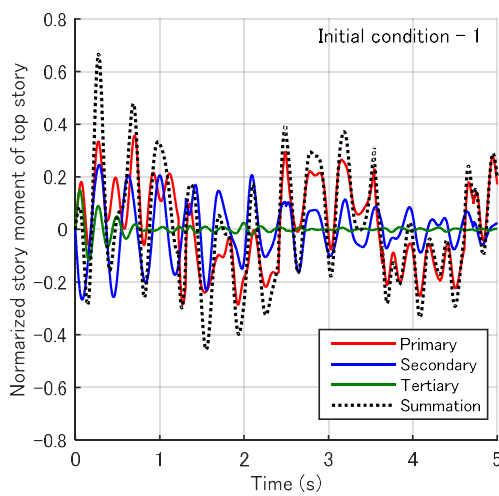

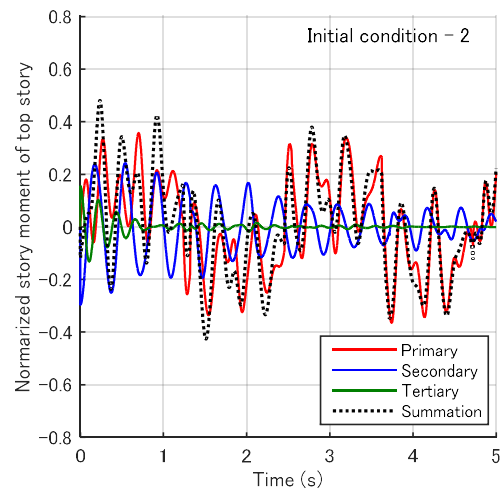(a) Initial condition - 1   (b) Initial condition - 2

Fig.11: Comparison of base shear coefficients under different initial conditions (CMFVA)

(a) Initial condition - 1   (b) Initial condition - 2

Fig.12: Comparison of normalized story moment of top story under different initial conditions (CMFVA)
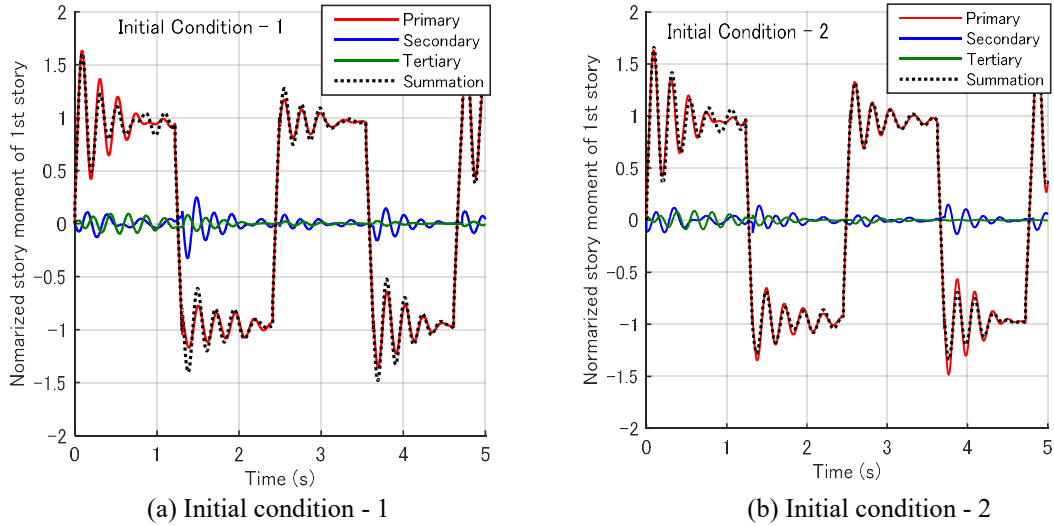
(a) Initial condition - 1   (b) Initial condition - 2

Fig.13: Comparison of normalized overturning moment under different initial conditions (CMFVA)

Figure 12 and 13 show normalized story moments, Ms_i, on the top and the base story which are calculated by the following equation, respectively. The story moment of the base story is the normalized overturning moment, M_{OVT}.

When $i<nst$,

$$Ms_i = \sum_{j=1}^{i} F_j \left(h_j - h_{i+1} \right) \bigg/ 0.5\, w \sum_{j=1}^{i+1} m_j \tag{11}$$

When $i=nst$,

$$Ms_i = M_{OVT} = \sum_{j=1}^{i} F_j h_j \bigg/ 0.5\, w \left(\sum_{j=1}^{i} m_j + m_{fb} \right) \tag{12}$$

where, i: number of story counted from the top, j: number of mass point counted from the top, nst: total number of stories, which is 10 in the case of the model shown in Fig.2, F_j: lateral force at the j-th math point, h_j: height of the j-th mass point, w: width of the system, m_{fb}: mass of footing beam.

As shown in Fig.12, the secondary and tertiary responses are relatively large in the story moment of the top story as well as in shear coefficients. In contrast, these responses become smaller in the overturning moment as shown in Fig.13. However, the overturning moment is amplified up to about 1.5 times static one by the vertical inertial effect explained in Fig.1.

Figure 14 shows time histories of base shear under the initial condition - 1 evaluated by the CMFVA comparing the uncoupled modal free vibration analysis (UCMFVA) which neglects "the coupling of N equations in modal coordinate" [16]. The results of the CMFVA and the UCMFVA are in good agreement. From the results shown in Fig 14. we can say that the secondary responses can be evaluated using the second natural mode of the contact phase. The primary response is more complicated than other responses because it is affected by higher modes arising from dynamic vertical motion. Figure 15 shows higher modes of the uplift phase which compose the primary response while the system is uplifting. These higher modes make the base shear fluctuate largely in this duration.
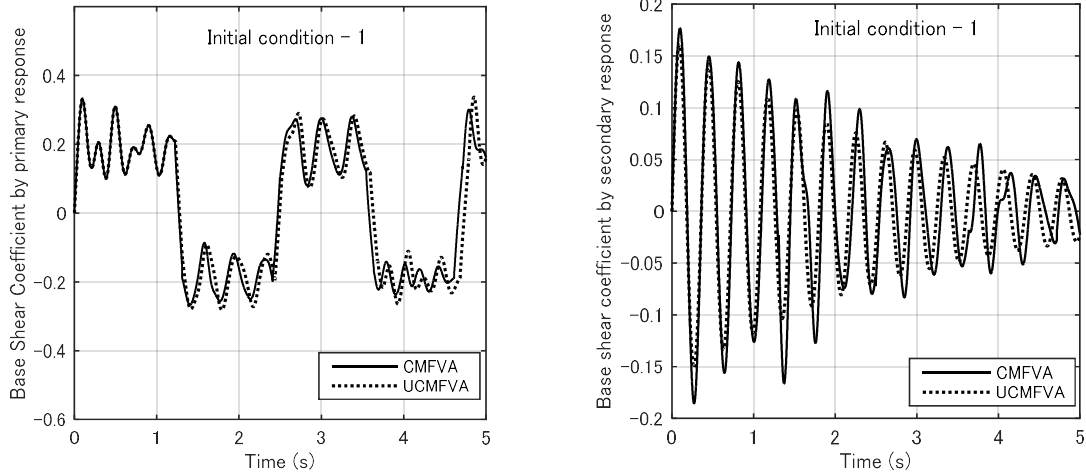
(a) Base shear coefficient by primary response　　　(b) Base shear coefficient by secondary response
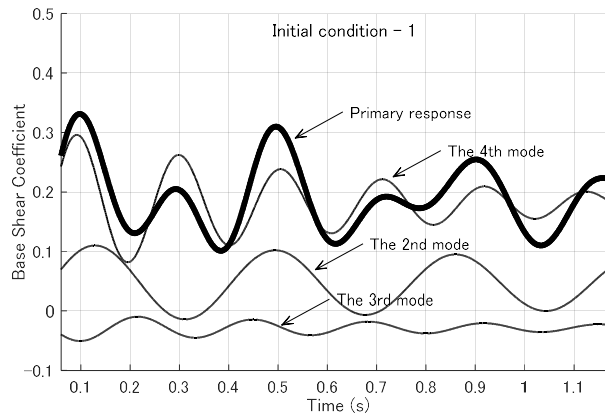
Fig.14: Comparison of CMFVA and UCMFVA

Figure 15: Higher modes composing the primary response for 0.1 - 1.1 sec. in Fig. 14

4　SIMPLIFIED MAXIMUM RESPONSE PREDICTION

To predict the maximum response values of the rocking system subjected to an earthquake ground motion simply, we suppose that they correspond to the maximum ones of free vibration responses. From the analysis results in the previous chapter, we can derive the following conclusions;

1) The maximum of primary response which is affected by higher modes arising from the dynamic vertical motion, which can be predicted by conducting the free vibration analysis under the first mode initial condition.

2) The maximums of secondary and tertiary responses are almost equal to those of systems in the contact phase which can be estimated by referring the response spectra of one mass system.

To predict the maximum responses, we need to combine the maximum ones of the primary, secondary and tertiary which are predicted by following the above-mentioned conclusions. In this study, we adopt the combination rule in the Steel Construction New Zealand guide in controlled rocking steel braced frames [17, 18]. The concept of this combination rule is expressed by the following equation.

$$R = R_P + \sqrt{R_2^2 + R_3^2} \qquad (13)$$

where, R: the maximum response, R_P: the maximum of the primary response, R_2: the maximum of the secondary response, R_3: the maximum of tertiary response.
The notation of Eq. (13) is changed for application in this study.

Figure 16 compares predicted values with the maximum values of a time history analysis in chapter 2 and those of free vibration analyses (CMFVA) in chapter 3. These figures show the results of story shear coefficients and story moments respectively. In the both figures, the predicted values tend to surpass all response values in the middle stories. However, we can say that the proposed method can provide reasonable prediction as a whole.
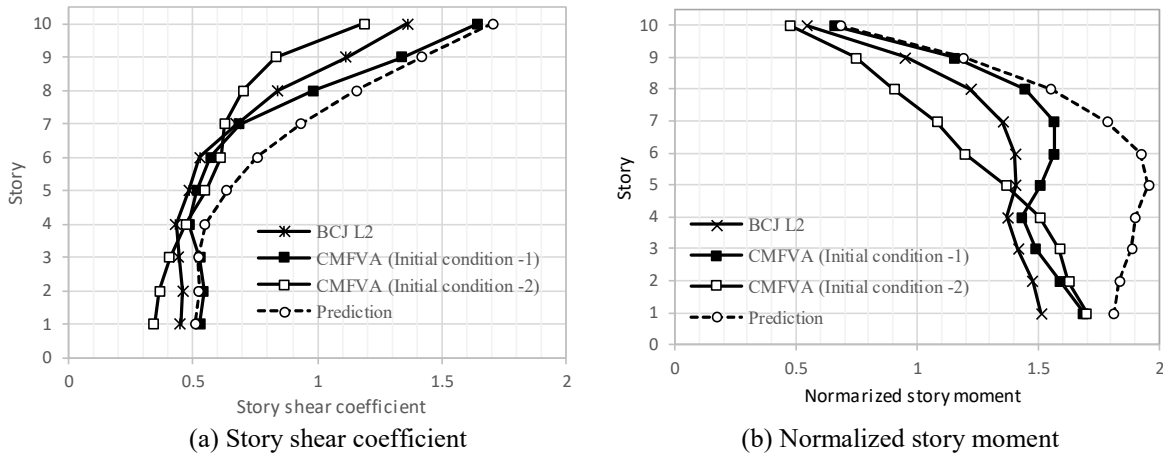

(a) Story shear coefficient (b) Normalized story moment
Figure 16: Comparison of predicted values with response values

5 CONCLUSIONS

To predict the maximum responses of the structures allowed to uplift, effects of higher modes were investigated by executing free vibration analyses. Free vibration responses were separated into the primary response, the secondary response and the tertiary response. Each separated response is determined by the corresponding modal initial condition.

The maximum of the primary response, which is affected by the higher modes arising from dynamic vertical motions during uplifting, can be predicted by a free vibration analysis under the first mode initial condition. The maximums of the secondary and the tertiary responses, which are amplified by high-frequency components of an earthquake ground motion, can be predicted by referring a response spectra of an earthquake ground motion.

Finally, it was presented that the maximum responses of the structures allowed to uplift can be predicted to combine the maximums of the three separated responses appropriately.

ACKNOWLEDGEMENT

REFERENCES

[1] J. W. Meek, *Effects of foundation tipping on dynamic response*, Journal of Structural Engineering, Vol.101, No.ST7, ASCE: 1297-1311, 1975.

[2]   A. Rutenberg, P. C. Jennings, G. W. Housner, *The response of Veterans Hospital Building 41 in the San Fernando Earthquake*, Earthquake Engineering and Structural Dynamic, 10(3), 359-379, 1982.

[3]   Y. Hayashi, *Damage reduction effect due to basement uplift of buildings*, Journal of Structural and Construction Engineering. AIJ 485, 53-62, 1996. (In Japanese)

[4]   Y. Hayashi, K. Tamura, M. Mori, I. Takahashi: *Simulation analysis of buildings damaged in the 1995 Kobe, Japan, earthquake considering soil-structure interaction*, Earthquake Engineering and Structural Dynamics, 28, 371-391, 1999.

[5]   R. W. Clough, A. A. Huckelbridge, *Preliminary experimental study of seismic uplift of a steel frame*, Report No.UBC/EERC-77/22. EERC, University of California, Berkeley, CA., 1977.

[6]   A. A. Huckelbridge, *Earthquake simulation tests of a nine story steel frame with columns allowed to uplift*, Report No.UBC/EERC-77/23. EERC, University of California, Berkeley, CA, 1977.

[7]   M. Midorikawa, T. Azuhata, T. Ishihara, A. Wada, *Shaking table tests on seismic response of steel braced frames with column uplift*, Earthquake Engineering and Structural Dynamics, 35(14), 1767-1785, 2006.

[8]   N. B. Chancellor, R. Sauce, J. M. Ricles, *Design and validation of steel self-centering concentrically-braced frames*, Proceeding of 16th WCEE, No. 2705, 2017.

[9]   E. Tahmasebi, R. Sause, J. M. Ricles, *Probabilistic Seismic Damage Analysis of Steel Self-Centering Concentrically Braced Frame Systems*, Proceeding of 16th WCEE, No. 2811, 2017.

[10] T. C. Steele, L. D. A. Wiebe, *Collapse Assessment of Controlled Rocking Steel Braced Frames with different of rocking joint parameters*, Proceeding of 16th WCEE, No. 2963, 2017.

[11] M. Midorikawa, N. Kotani, T. Okazaki, T, Asari, T. Ishihara, T. Azuhata, *Seismic energy response of multi-story steel rocking frames allowing column mid-height at the first story*, Proceeding of 16th WCEE, No. 2986, 2017.

[12] M. Kovacs, L. Wiebe, *Controlled rocking heavy timber walls for regions of low to moderate seismicity*, Proceeding of 16th WCEE, No. 3253, 2017.

[13] J. Binder, C. Christopoulos, M. Gray, *Seismic response of hybrid ductile-rocking buckling restrained braced frames with cast steel supplement energy dissipation element*, Proceeding of 16th WCEE, No. 4450, 2017.

[14] T. Ishihara, M. Midorikawa, T. Azuhata, *Modal analysis of uplifting behavior of buildings modeled as uniform shear-beam*, Proceeding of 14th WCEE, Paper ID 05-06-0116, 2008.

[15] T. Ishihara, M. Midorikawa, T. Azuhata, *Modal properties and free vibration of uplifting behavior of multistory buildings modeled as uniform shear-beam*, Journal of Structural and Construction Engineering. Vol. 74, AIJ 640, 1055-1061, 2009. (In Japanese)

[16] A. K. Chopra, R. K. Goel: *A modal pushover analysis procedure for estimating seismic demands for buildings*, Earthquake Engineering and Structural Dynamics, 31, 561-582, 2002

[17] L. Wiebe, G. Sidwell, S. Gledhill, *Design guide for controlled rocking steel braced frames*, Steel Construction New Zealand, Manukau City, New Zealand, 2015.

[18] T. C. Steele, L. D. A. Wiebe, *Dynamic and equivalent static procedures for capacity design of controlled rocking steel braced frames*, Earthquake Engineering and Structural Dynamics, 45, 2349-2369, 2016.